mater.scichina.com link.springer.com

Published online 2 November 2022 | https://doi.org/10.1007/s40843-022-2225-x
Sci China Mater 2023, 66(3): 964–973

Flexible freestanding conductive nanopaper based on PPy:PSS nanocellulose composite for supercapacitors with high performance

Yue Liang[1], Zhen Wei[2], Hung-En Wang[1], Ruigang Wang[2*] and Xinyu Zhang[1*]

ABSTRACT A freestanding, binder-free flexible polypyrrole: polystyrene sulfonate/cellulose nanopaper (PPy:PSS/CNP) electrode is successfully fabricated by a low-cost, simple, and fast vacuum filtration method for the first time. The hierarchical structure of CNP with high surface area and good mechanical strength not only provides a high electroactive region and shortens the diffusion distance of electrolyte ions, but also mitigates the volumetric expansion/shrinkage of the PPy during the charging/discharging process. The optimized PPy:PSS/CNP exhibits a high areal specific capacitance of 3.8 F cm^{-2} (corresponding to 475 F cm^{-3} and 240 F g^{-1}) at 10 mV s^{-1} and good cycling stability (80.9% capacitance retention after 5000 cycles). The cyclic voltammetry curves of PPy:PSS/CNP at different bending angles indicate prominent flexibility and electrochemical stability of the electrode. Moreover, a symmetric supercapacitor device is assembled and delivers a high areal energy density of 122 μW h cm^{-2} (15 W h cm^{-3}) at a power density of 4.4 mW cm^{-2} (550 mW cm^{-3}), which is superior to other cellulose-based materials. The combination of high supercapacitive performance, flexibility, easy fabrication, and cheapness of the PPy: PSS/CNP electrodes offers great potential for developing the next generation of green and economical portable and wearable consumer electronics.

Keywords: cellulose nanopaper, conducting polymer, binder-free, flexible electrode, supercapacitor

INTRODUCTION

Supercapacitors, a type of energy storage systems, have attracted enormous attention from the academic and industry communities due to the fast charge-discharge rate, long cycling life, good operational safety, and high power density [1,2]. With the boosted development of rechargeable consumer electronics, portable and wearable electronic devices rapidly appear in our life such as roll-up displays and smart textiles, and the flexible supercapacitor market has become an emerging field. In general, flexible supercapacitors not only need to meet the fundamental standard of the conventional capacitors but also possess promising properties including lightweight and extra mechanical flexibility [3,4]. In the past few years, many researchers have focused on fabricating the flexible supercapacitors with high electrochemical performance. Nevertheless, the challenges originating from the intended end-use exist such as the high cost of raw materials, flexibility, complicated fabrication procedures, and toxicity, and the screening of the substrate with high conductivity still needs to be overcome [5]. Therefore, the development of flexible supercapacitors with low cost, light weight, good mechanical properties, environmental friendliness, and outstanding electrochemical properties is desired.

As the central component of a flexible supercapacitor, flexible electrodes are considered to have a key impact on the performance of the flexible supercapacitors. Polypyrrole (PPy) as a kind of conductive polymer has been extensively studied as a promising component of electrode materials due to its low cost, environment-friendliness, facile and simplistic preparation, good redox property, and high theoretical specific capacitance [6,7]. Nevertheless, the poor conductivity, low solubility in common solvents and the instable structure of PPy have limited its practical application. To address these issues, numerous strategies have been applied to modify the interconnected microstructure and improve the performance of PPy. One typical strategy is to blend or composite PPy with highly conductive carbon-based materials (i.e., active carbon (AC), carbon nanotube (CNT), and graphene) to cushion the molecular chain damage of PPy during the repeated adsorption/desorption of electrolyte ions [8,9]. In addition, polymeric surfactants with different sulfonating groups have been used as additives to improve the thermal and mechanical stabilities, solubility and dispersity, and electric conductivity of PPy during the polymerization process [10,11]. Especially, the water soluble sulfonated polymeric surfactant (polystyrene sulfonate (PSS)) with excellent mechanical flexibility and tunable electrical conductivity has attracted intense attention among various surfactants [12–14]. For instance, nanocolloidal PPy:PSS composites were prepared through a dispersion polymerization technique by Maruthamuthu *et al*. [15]. The conductivity and solubility of PPy were easily controlled by the concentrations of PSS. When the weight ratio of PSS was 15% with pyrrole, the product exhibited improved dispersion, a higher dielectric constant, and relatively low dielectric loss. Although the water-dispersible and conductivity properties of PPy have been effectively improved, the lack of the ability to form stable chemical bonds and entangled networks made them easily broken and difficult to form films. Moreover, the fabrication of flexible supercapacitor electrodes usually needs binder, conductive additive, and current collector. However, these constituents would increase the weight and resistance of the electrode, and reduce the accessible surface of the electrode. Therefore, many efforts should be focused on

[1] Department of Chemical Engineering, Auburn University, Auburn, AL 36849, USA
[2] Department of Metallurgical and Materials Engineering, The University of Alabama, Tuscaloosa, AL 35487, USA
* Corresponding authors (emails: xzz0004@auburn.edu (Zhang X); rwang@eng.ua.edu (Wang R))

developing freestanding, binder-free flexible thin film electrodes which can also function as current collectors themselves displaying high electrochemical performance and good mechanical properties.

Cellulose nanofiber (CNF) existing in cell walls of plants is the most abundant natural polymer on earth and is considered as a promising alternative advanced material for the next generation petroleum-based materials, with outstanding features including abundant raw material, low-cost production, high specific surface area, great biocompatibility and biodegradability [16,17]. Recently, CNFs are considered promising supporting substrates for energy storage devices. The flexible conducting film electrode of multi-walled CNT (MWCNT)/poly(3,4-ethylenedioxythiophene):PSS/cellulose (MCPP) prepared by supramolecular assembly showed a high specific capacitance (485 F g^{-1}, at 1 A g^{-1}) and good cycling stability (95% initial capacitance remained after 2000 cycles) [18]. The freestanding electrode PPy/functionalized CNTs (f-CNT)/cellulose composite films were prepared through a facile and green freeze-and-thaw process, where the f-CNTs and cellulose as matrices not only provided a large interfacial area for the storage/release of charge carriers, but also formed a porous structure through interfacial hydrogen bonding between the f-CNTs and cellulose to provide charge transfer channels. The as-prepared composites exhibited high areal capacitance (2147 mF cm^{-2} at 1 mA cm^{-2}) and outstanding cycling stability [19].

In this work, a low-cost and environmentally friendly nanocellulose was chosen as the support substrate to synthesize the freestanding, binder-free flexible PPy:PSS/CNF nanopaper (PPy:PSS/CNP) electrode by a simple and fast vacuum filtration method. Considering the practical applications, the mechanical and electrochemical properties of the electrodes were adjusted by controlling the weight ratio of PPy:PSS and CNF. The optimized PPy:PSS/CNP exhibited a high areal specific capacitance, good cycling stability, and prominent flexibility. Moreover, a symmetric supercapacitor device was assembled and delivered a high areal energy density of 122 μW h cm^{-2} (15 W h cm^{-3}) at a power density of 4.4 mW cm^{-2} (550 mW cm^{-3}), which was better than those of supercapacitors based on other cellulose materials. In light of high supercapacitive performance, flexibility, low cost, and ease of large-scale manufacturing, the PPy:PSS/CNP electrode has a promising application in the next generation of green, economical portable and wearable consumer electronics.

EXPERIMENTAL SECTION

Materials

The CNFs were purchased from the University of Maine (Lot no-U31, 3 wt%, grade-91% fines). Pyrrole monomer (99%) was obtained from Tokyo Chemical Industry. PSS (99%) was purchased from Acros, USA. Ammonium peroxydisulfate (APS, 98%) was purchased from Alfa Aesar. Sulfuric acid (H_2SO_4, 95%–98%) and hydrochloric acid (HCl, 36.5%–38%) were acquired from VWR, USA. All the chemicals were directly used without any purification.

Preparation of CNP

The CNP was prepared by a simple vacuum filtration method according to our previous work [20]. Briefly, the CNFs suspension was diluted to a concentration of 0.5 wt% with 1 mol L^{-1} HCl. The diluted CNFs suspension (40 mL) was continuously stirred for 2 h, and then a well dispersed suspension was obtained. Subsequently, the suspension was filtered using a polypropylene filter membrane (diameter of 10 cm, pore size of 0.45 μm). Another polypropylene filter membrane was used to cover the wet CNFs film and dried using a hot plate at 105°C for 2 h to obtain the CNP.

Preparation of PPy:PSS/CNP

The schematic formation of PPy:PSS/CNF composites is shown in Scheme 1. In a typical synthesis process, 40 mL of CNFs suspension (0.5 wt%) and 20 mL 1 mol L^{-1} HCl were added to a reaction vessel and stirred for 30 min to form a well-dispersed suspension. Then pyrrole monomer and PSS were dissolved into the mixture and stirred for another 10 min. Next, APS as an oxidant, was added to initiate the polymerization of pyrrole. The polymerization was carried out for 3–4 h at room temperature under constant magnetic stirring. The as-synthesized PPy:PSS/CNF composite was centrifuged and washed several times with deionized water. Later, the product was diluted to 200 mL with deionized (DI) water and sonicated for 5 min at a power input of 500 W. Finally, the PPy:PSS/CNF suspension was filtered using a polypropylene filter membrane (diameter of 10 cm, pore size of 0.45 μm) by vacuum filtration. Another polypropylene filter membrane was used to cover the wet PPy:PSS/CNF film and dried using a hot plate at 105°C for 2 h to obtain the PPy:PSS/CNP. The weight percentage of PPy:PSS in the PPy:PSS/CNP was calculated following Equation (1):

$$\text{Weight ratio} = (m - 0.2/m) \times 100\%, \quad (1)$$

where m is the dry weight (g) of the PPy:PSS/CNP.

In order to obtain optimal performance of composites, different weight ratios of PPy:PSS in PPy:PSS/CNP were adjusted. The details are given in Table 1.

Tensile test

Tensile test was carried out by a TA instrument dynamic mechanical analyzer RSA III with the ASTM standard D882-18 test method. The samples with 1 cm (width) × 5.5 cm (length) dimension were used to test. The crosshead speed was 6 mm min^{-1} and the gauge length was 15 mm. The data were obtained by averaging three measurements for each sample.

Conductivity measurement

The sheet resistance (R_s) was measured on square specimens (1.5 cm × 1.5 cm) by the four-point probe method using a digital multimeter (RIGOL DM3068). The average value was calculated after five measurements for each sample. The conductivity (ρ, S m^{-1}) was calculated based on Equation (2) shown as follows [21]:

$$\rho = 1/(R_s \times t), \quad (2)$$

where t is the thickness of the film in centimeter and R_s is the resistance in Ohm.

Electrochemical measurements

The electrochemical measurements were carried out using a CHI electrochemical workstation (CHI 760D) in three-electrode and two-electrode systems at room temperature and all the tests were performed in 1 mol L^{-1} H_2SO_4. For the three-electrode system, the Ag/AgCl electrode, platinum sheet (1 cm × 1 cm) and PPy:PSS/CNP (1 cm × 1 cm × 0.08 mm, about 15.8 mg) were used as the reference electrode, the counter electrode, and the working

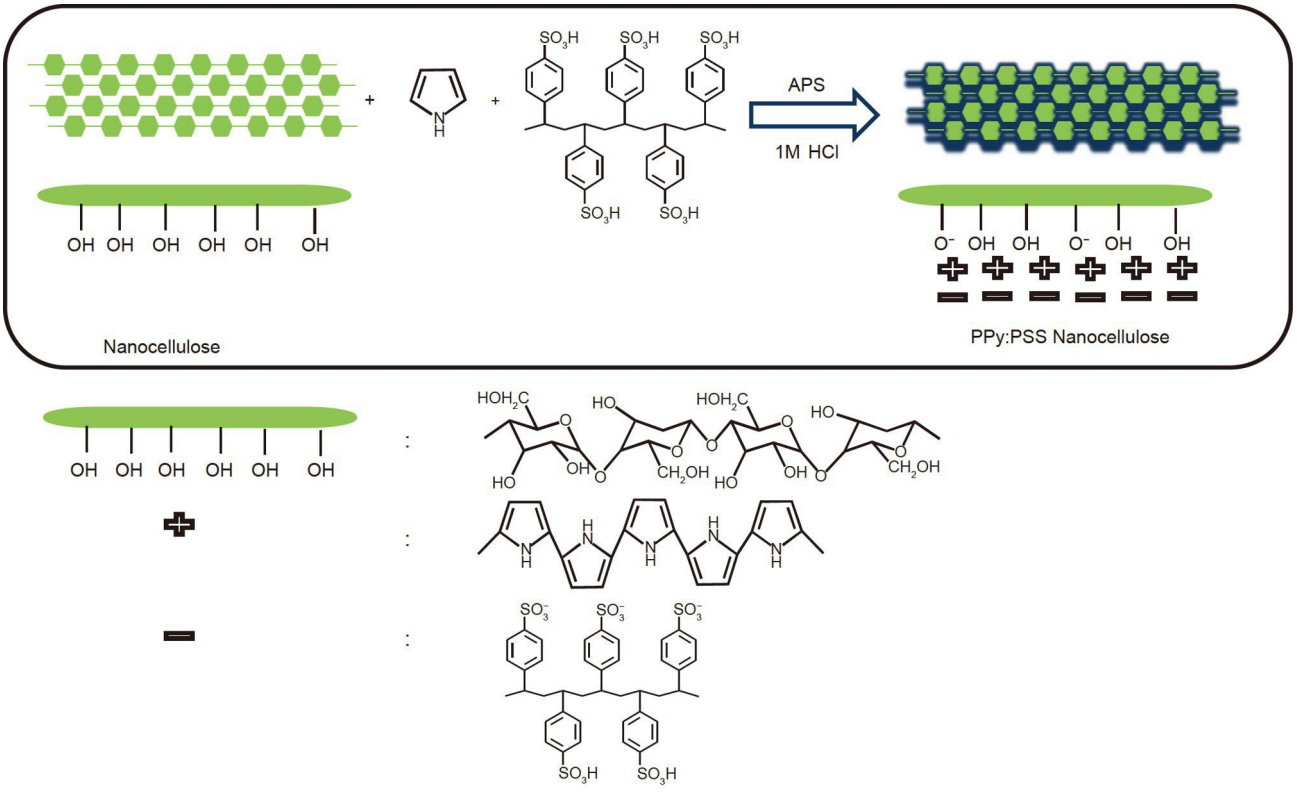

Scheme 1 The schematic formation of PPy:PSS/CNF composites.

Table 1 Operation conditions for synthesizing PPy:PSS/CNP

Sample	CNF (g)	Pyrrole (mL)	PSS (g)	APS (g)	Weight ratio of PPy:PSS (%)
PPy:PSS/CNP-1	0.2	0.1	0.0097	0.228	9.5 ± 0.5
PPy:PSS/CNP-2	0.2	0.2	0.0194	0.456	30.6 ± 1.1
PPy:PSS/CNP-3	0.2	0.3	0.0291	0.684	44.8 ± 1.5
PPy:PSS/CNP-4	0.2	0.4	0.0388	0.912	54.1 ± 2.0
PPy:PSS/CNP-5	0.2	0.5	0.0485	1.140	61.6 ± 2.3

electrode, respectively. Cyclic voltammetry (CV) and galvanostatic charge/discharge (GCD) curves were measured at the potential window of −0.2–0.8 V. The electrochemical impedance spectroscopy (EIS) analysis was conducted at open-circuit voltage using alternating current amplitude of 0.005 V in the frequency range of 10^{-1} to 10^{5} Hz. The stability tests were performed on an Arbin Instrument (version 4.21). The symmetric supercapacitor was fabricated by two pieces of film (1 cm × 1 cm × 0.08 mm, about 16 mg) and tested in the two-electrode system. CV and GCD curves were recorded over the potential window of 0–1 V. The areal specific capacitances (C_A, F cm^{-2}) of electrode can be estimated by Equation (3) [22],

$$C_A = \int I dV/A\Delta Vs, \quad (3)$$

where I is the discharging current (A), $\int I dV$ is the integrated area of CV curve, A is the area of the electrode (cm^2), s is the scan rate (V s^{-1}), and ΔV is the potential window (V). For the gravimetric capacitance (C_g, F g^{-1}) and the volumetric capacitance (C_V, F cm^{-3}), the area in the formula needed to be replaced by the volume or mass of the electrode, respectively. The energy density was the amount of energy stored per mass/unit volume of the active material. For a full device, the energy density and power density were two key parameters to evaluate the overall performance of a supercapacitor. The areal energy density (E, W h cm^{-2}) was obtained by

$$E = C_A\Delta V^2/(2 \times 3600). \quad (4)$$

The energy released per unit time was the power density, which was used to evaluate the speed of the charge and discharge.

$$P = (3.6 \times E \times s)/\Delta V, \quad (5)$$

where P was the power density (W cm^{-2}). For the volumetric energy density (W h cm^{-3}), the area in the formula needed to be replaced by the volume of the electrode.

Materials characterization

Scanning electron microscopy (SEM; Apreo FE) was used to confirm the morphologies of the samples. The compositional elements were investigated by energy dispersive X-ray spectroscopy (EDS; EDAX Instruments). Fourier transform infrared (FTIR) spectra were measured on a Nicolet 6700 using KBr disk in the wavenumber range of 400–4000 cm^{-1}.

RESULTS AND DISCUSSION

Materials characterization

FTIR analysis provides insight into the molecular structures of CNP, PPy:PSS, and PPy:PSS/CNP, as shown in Fig. 1. In the spectrum of pure CNP, the bands at 1764, 1616, 1430, 1313, 1161, 1105, 1050, and 894 cm^{-1} were attributed to the stretching of C=O bonds, bending mode of the absorbed water, symmetric bending of $–CH_2$, C–O symmetric stretching, the asymmetric stretching of C–O, C–OH skeletal vibration, pyranose C–O–C stretching, and C–H deformation vibrations out of plane of aromatic ring, respectively [23]. The characteristic vibrational bands of PPy:PSS presented at 1542, and 1440 cm^{-1} corresponding to the stretching of C–C and C–N in the pyrrole ring, respectively. The peak exhibited at 1310 cm^{-1} was assigned to the deforming vibrations of C–H and N–H. The doping state of PPy was confirmed by the peaks at 1170 and 960 cm^{-1}. The absorption peak at 1033 cm^{-1} was due to the sulfur dioxide (SO_2) group stretching vibrations [14,15,24]. For PPy:PSS/CNP, the FTIR spectra retained the typical characteristic peaks of PPy:PSS and the cellulose peaks almost disappeared, indicating the PPy:PSS was homogeneously coated on the surface of CNFs. Moreover, all the major peaks shifted to the lower frequency, suggesting that the hydrogen bonding formed between CNFs and PPy:PSS. These results confirmed the successful formation of PPy:PSS/CNP.

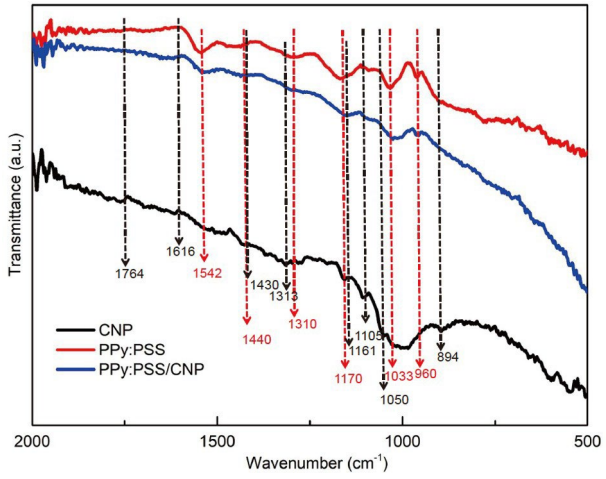

Figure 1 FTIR spectra of CNP, PPy:PSS, and PPy:PSS/CNP.

The surface and cross-sectional morphology of the pure CNP and PPy:PSS/CNP were examined by SEM under different magnifications. As revealed in Fig. 2a, the pure CNP exhibited a smooth surface and randomly entangled CNFs. The cross-sections showed a compact multilayer configuration that was formed by CNFs tightly entangled with each other through the strong hydrogen bonding (Fig. 2b, c). These abundant hydrogen bonds provided strong interactions between layers, which reflected the high mechanical properties of CNP. After the introduction of PPy:PSS, the PPy:PSS particles were tightly attached to the surface of CNP, which was mainly due to the hydrogen bonds formed between CNFs and PPy chains, leading to a rougher surface of PPy:PSS/CNP than the pure CNP (Fig. 2d). Besides, EDS proved the existence of sulfur (S) element in PPy:PSS/CNP, further indicating the successful introduction of PPy:PSS on the surface of CNP (Fig. S1). Compared with the pure CNP, the cross-sectional morphology of PPy:PSS/CNP displayed obviously expanded interior lamellar structures and slightly loose structure, which was due to the PPy:PSS within the CNP interrupting the interfibrillar hydrogen bond among CNFs and the refilled PPy:PSS particles enlarging the distance among CNFs (Fig. 2e, f). The loose structure was expected to favor the electronic transfer and improve the electrochemical performance of the active electrode materials.

Mechanical property

The stress *vs*. strain curves and tensile properties of the pure CNP and PPy:PSS/CNP are shown in Fig. 3a, b. Compared with the pure CNP, the tensile mechanical response of PPy:PSS/CNP decreased distinctly after introducing PPy:PSS. This result might mainly be due to the disruption of the original CNFs connecting

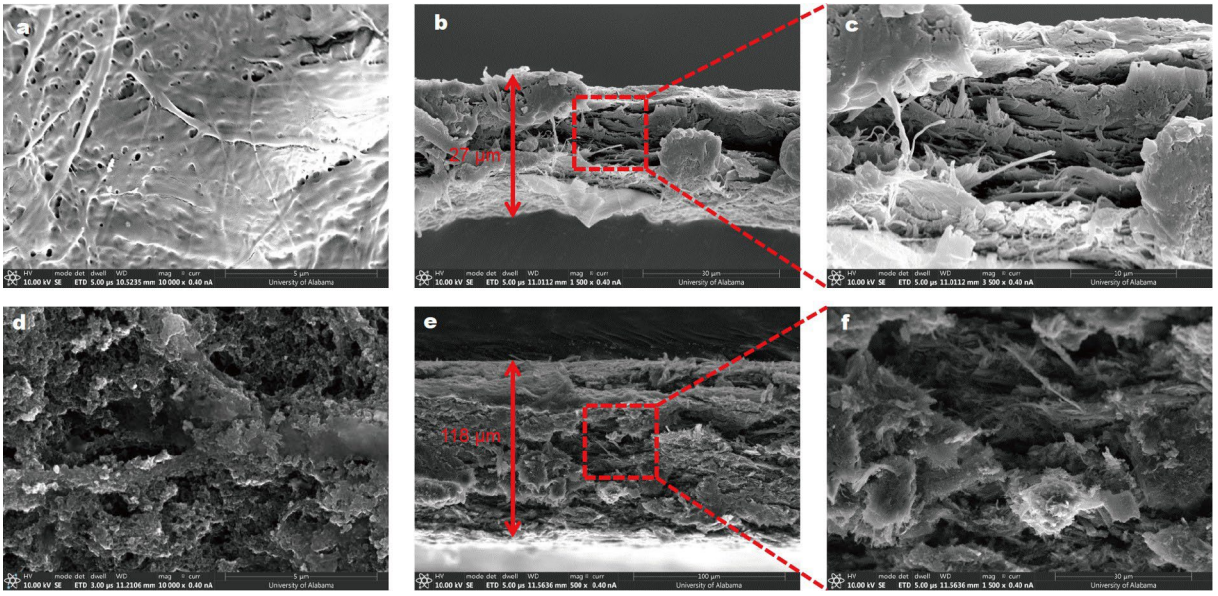

Figure 2 SEM surface and cross-section images of (a–c) pure CNP, and (d–f) PPy:PSS/CNP.

network and the formation of new hydrogen bonds between PPy:PSS and CNFs. It was clear that the connection between the PPy:PSS and CNFs was weaker than the hydrogen bonding interaction among CNFs in CNP, leading to diminished mechanical properties of PPy:PSS/CNP. In addition, the number of intermolecular and intramolecular hydrogen bonds in nanocellulose would be reduced due to the presence of negatively charged PSS (SO^{3-}) between nanocelluloses [25]. As the weight ratio of PPy:PSS increased, the tensile strength and elongation at break of PPy:PSS/CNP reduced from 42.6 to 9.9 MPa and from 10.2% to 6.9%, respectively, since the larger amount of PPy:PSS incorporated into the CNP, the fewer the CNF interfibrils connections. This result evidenced that the mechanical properties of PPy:PSS/CNP were affected by the number of hydrogen bonds between fibers. Interestingly, even the weight ratio of PPy:PSS reached 54.1%, the PPy:PSS/CNP strip with the width and thickness of 10 and 0.08 mm, could still lift up a static load of 800 g. Compared with other conductive polymer/CNF composites, our work presented good mechanical nature [20,21,25–27]. It implied that nanocellulose was a promising substrate for the preparation of flexible electrodes.

Conductivity

As shown in Fig. 4a, the electrical conductivity of PPy:PSS/CNP increased continuously with the increasing amount of PPy:PSS. When the weight ratio of PPy:PSS was 61.6%, the conductivity reached 5.776 S cm^{-1}, which suggests that the conductivity of PPy:PSS/CNP was mainly attributed to the content of PPy:PSS. However, despite a high mass loading of conductive active material could improve the supercapacitor performance, the poor mechanical strength nature of PPy:PSS/CNP-5 that might limit its practical application still should be considered. It is worth noting that even the mass loading of PPy:PSS was reduced to 54.1%, the PPy:PSS/CNP could still exhibit high conductivity of 4.456 S cm^{-1} in this work, which was higher than those of many similar conductive composites reported previously, such as PPy/CNF (0.26 S cm^{-1}), CNF/poly(3,4-ethylenedioxythiophene) (PEDOT):PSS (2.58 S cm^{-1}), and PPy/acrylic acid (AA) grafted nanocrystal cellulose hydrogel (PPy/NCC-g-AA) (8.8×10^{-3} S cm^{-1}) [21,25,28]. Fig. 4b demonstrated that PPy:PSS/CNP-4 as a connecting lead could light a light-emitting diode (LED) bulb very well under different bending angles, suggesting their splendid conductance stability and flexibility.

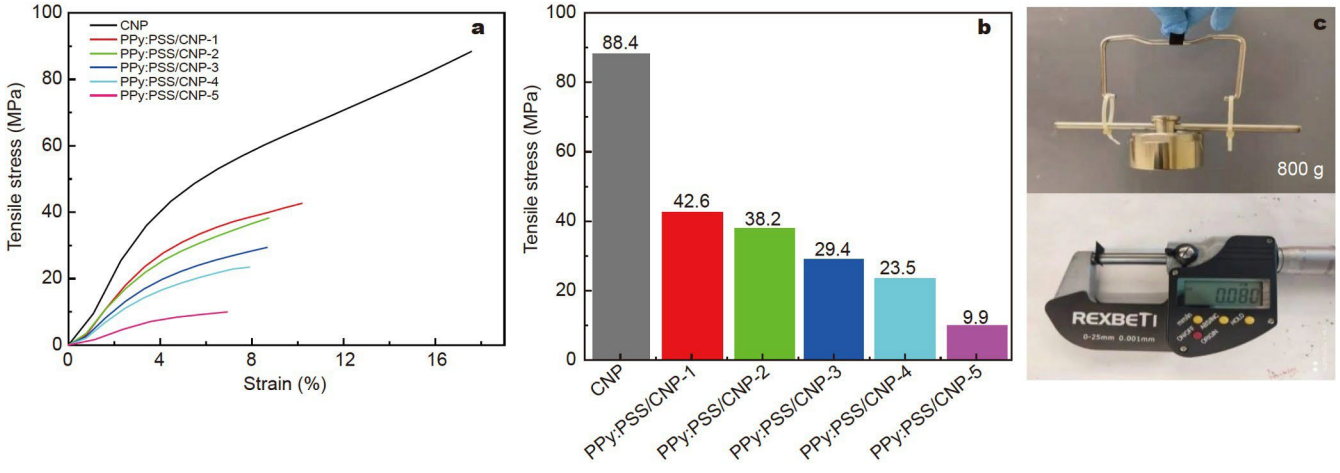

Figure 3 (a) Stress *vs.* strain plots and (b) tensile strengths for CNP and PPy:PSS/CNP with different PPy:PSS mass loadings. (c) Snapshots of PPy:PSS/CNP-4 strip, which can lift up a static load of 800 g.

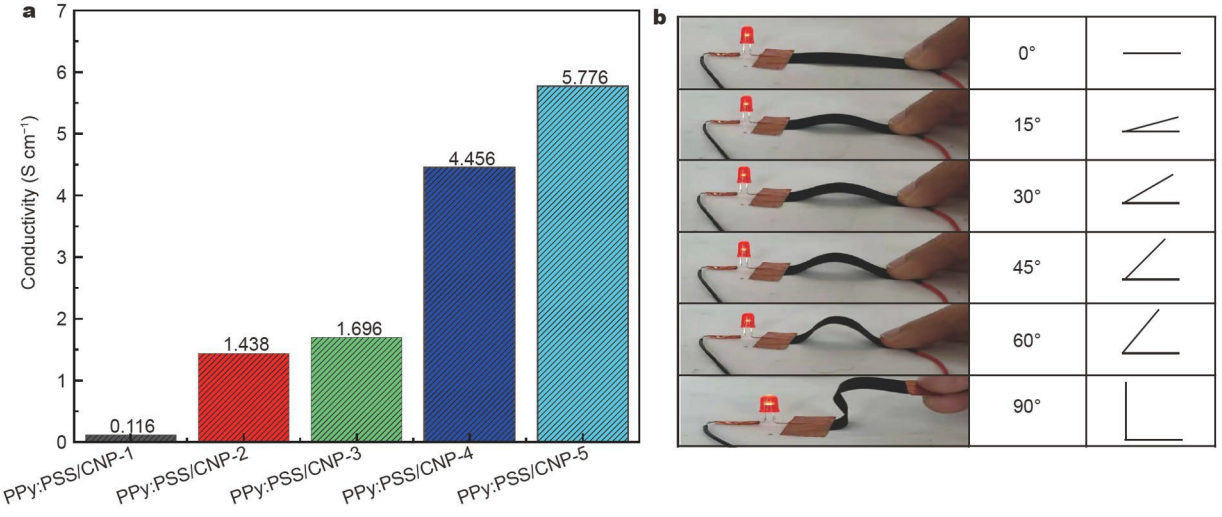

Figure 4 (a) Conductivities and (b) photographs of PPy:PSS/CNP-4 films with different bending angles.

Combining with the results of the mechanical strength of PPy:PSS/CNP-4, it was considered as an optimal electrode candidate used for the electrochemical test.

Electrochemical characterization

Fig. 5a presents the CV curves of PPy:PSS/CNP-4 at various scan rates. A quasi-rectangular shape was exhibited under lower scan rates, corresponding to a good pseudocapacitive response. With the increasing scan rates, the curves distorted into a leaf-like shape. The deviation of CV curves was mainly due to the controlled ion diffusion process impeding the accessibility of ions and active sites and causing the charge collection at the solid/liquid interface, which increased the internal diffusion resistance of the electrode. There are no obvious redox peak observed, suggesting that the fast electron and ion transfer throughout the electrodes [29–31]. The charge-discharge performance of PPy:PSS/CNP-4 is shown in Fig. 5b. All the GCD curves were found to be nearly triangular shapes with a very small voltage drop, indicating superior pseudocapacitive behavior and excellent reversibility of ion transfer and diffusion properties for the electrode. Based on the CV curves, the specific capacitances for the area, volume, and weight were calculated as shown in Fig. 5c, d. The maximum specific capacitance value was 3.8 F cm^{-2} (475 F cm^{-3}, 240 F g^{-1}) at 10 mV s^{-1}. Compared with other cellulose-based conductive nanopapers in Table 2, our work had a highest value. From 10 to 40 mV s^{-1}, 62% of initial area capacitance was retained. The loss of capacitance could be explained by the increase of the internal resistance due to the diffusion limitations of the electrolyte ions into the electrode material which could not match the rate of the electron transfer of the electrode materials. The superior rate performance of PPy:PSS/CNP-4 was ascribed to the high conductivity of PPy and the synergistic effect between PPy:PSS and CNFs, which could lower the interfacial charge-transfer resistance and facilitate the transportation of electrons. EIS was conducted to analyze the intrinsic charge storage of the electrode. As displayed in Fig. 5e,

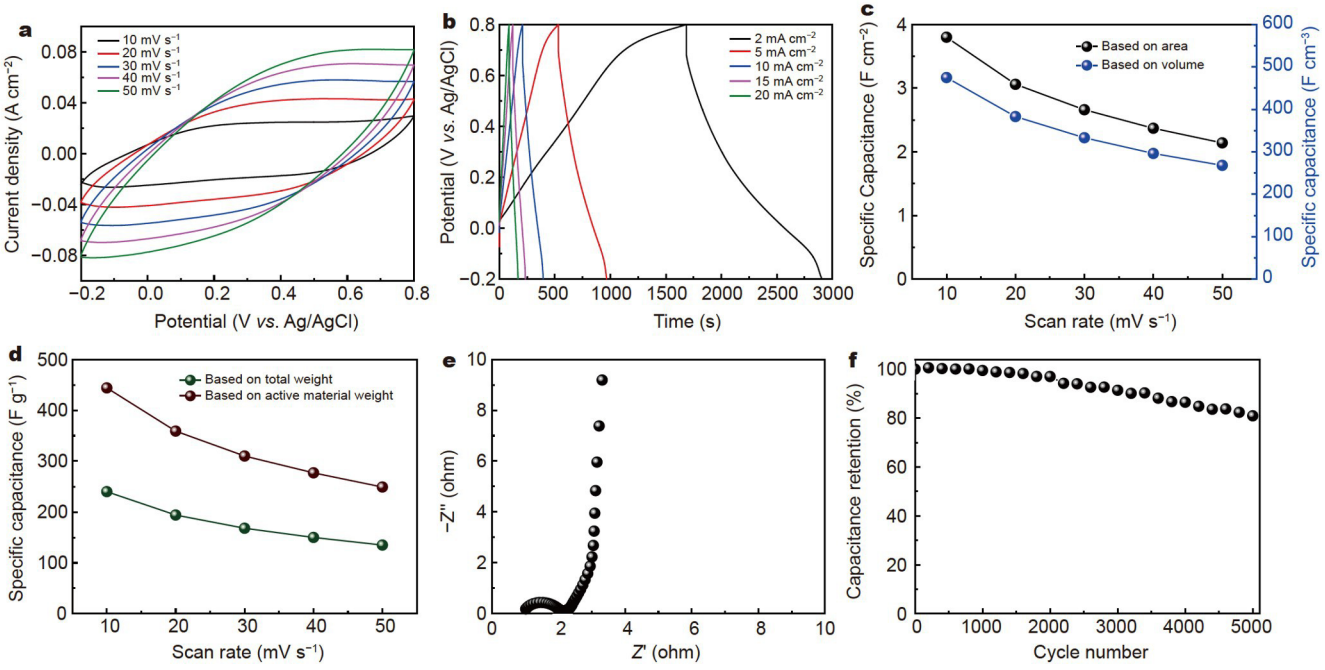

Figure 5 The electrochemical performance of the PPy:PSS/CNP-4 electrode in 1 mol L^{-1} H_2SO_4 electrolyte. (a) CV curves; (b) GCD curves; (c) specific capacitance based on areal and volume as functions of current density; (d) specific capacitance based on total weight and active material weight as functions of current density; (e) Nyquist plot; (f) cycling stability at 10 mA cm^{-2}.

Table 2 Comparison of the PPy:PSS/CNP electrode with reported electrodes based on nanocellulose-supported conductive materials

Electrode materials	Specific capacitance	Capacitance retention (cycles)	Ref.
CNF/CNT/PANI[a]	315 F g^{-1}, at 1 A g^{-1}	92.0% (10,000)	[33]
CF[b]-CNF/AC/MWCNT	1.74 F cm^{-2}, at 1 mA cm^{-2}	96.7% (3000)	[34]
PPy/rGO[c]/CNF	304 F g^{-1}, at 0.5 A g^{-1}	81.8% (1000)	[35]
PPy/cellulose	129.6 F g^{-1}, at 0.48 A g^{-1}	99.3% (7000)	[36]
rGO/cellulose	212 F g^{-1}, at 0.5 A g^{-1}	94.0% (14,000)	[37]
PEDOT/cellulose paper	115 F g^{-1}, at 1 A g^{-1}	91.0% (2500)	[38]
PEDOT:PSS/CNP	854.4 mF cm^{-2} (106.8 F cm^{-3}, 159.7 F g^{-1}), at 5 mV s^{-1}	95.5% (10,000)	[20]
PPy/GR/CNF	264.3 F g^{-1}, at 0.25 A g^{-1}	85.7% (1000)	[39]
PPy:PSS/CNP	3.8 F cm^{-2} (475 F cm^{-3}, 240 F g^{-1}) at 10 mV s^{-1}	80.9% (5000)	This work

a) PANI: polyaniline; b) CF: carbon fiber; c) rGO: reduced graphene oxide.

the Nyquist plot showed a small semicircle in the high-frequency region related to the charge transfer resistance of the electrode and a straight line in the low-frequency region corresponding to Warburg impedance reflecting the capacitive behavior of the electrode. This observation further proved that the PPy:PSS/CNP-4 electrode possesses a low charge transfer resistance and a fast charge transfer rate performance. Moreover, PPy:PSS/CNP-4 demonstrated remarkable cycling stability (80.9% capacitance retention after 5000 cycles) due to the incorporation of the cellulose network with good mechanical strength that could effectively overcome the shortcomings of the volume expansion/shrinkage for PPy during the charging/discharging processes (Fig. 5f). The mechanical properties of PPy:PSS/CNP-4 were further evaluated after the cycling stability test (5000 cycles) in the three-electrode system. As displayed in Fig. S2, the tensile stress of PPy:PSS/CNP-4 decreased remarkably from 23 to 4.8 MPa. The decreasing tensile stress for PPy:PSS/CNP-4 might be mainly attributed to the water molecule that interrupts the hydrogen bond among composites [32]. Fig. 6a, b present the CV curves and digital photos of PPy:PSS/CNP-4 at different bending angles. The CV curves show a minimal deformation, further demonstrating the stable performance of the electrode.

To evaluate the practical application of the PPy:PSS/CNP-4 film electrode, the electrochemical characterization of the symmetric supercapacitor that was assembled by two pieces of PPy:PSS/CNP-4 electrodes (1 cm × 1 cm) was performed (Fig. 7a).

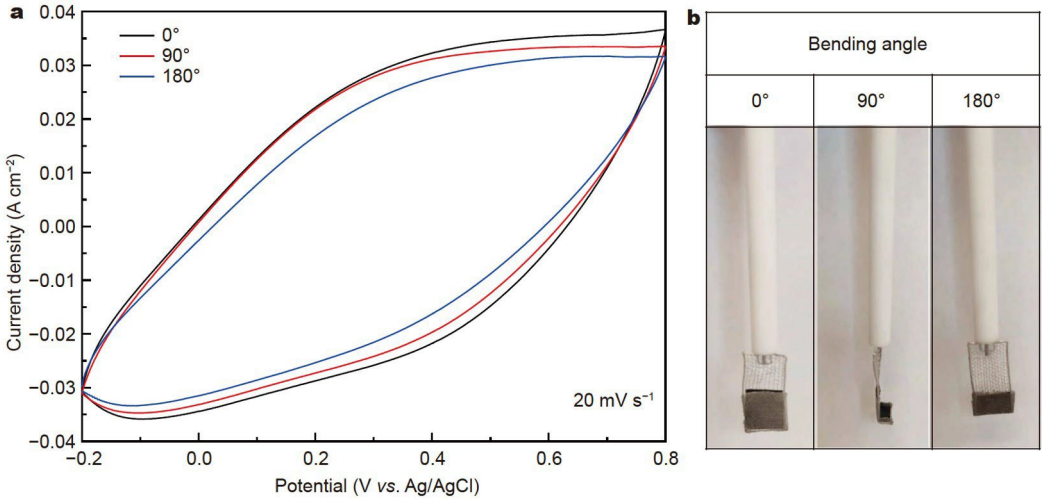

Figure 6 (a) CV curves and (b) digital photos of PPy:PSS/CNP-4 at different bending angles.

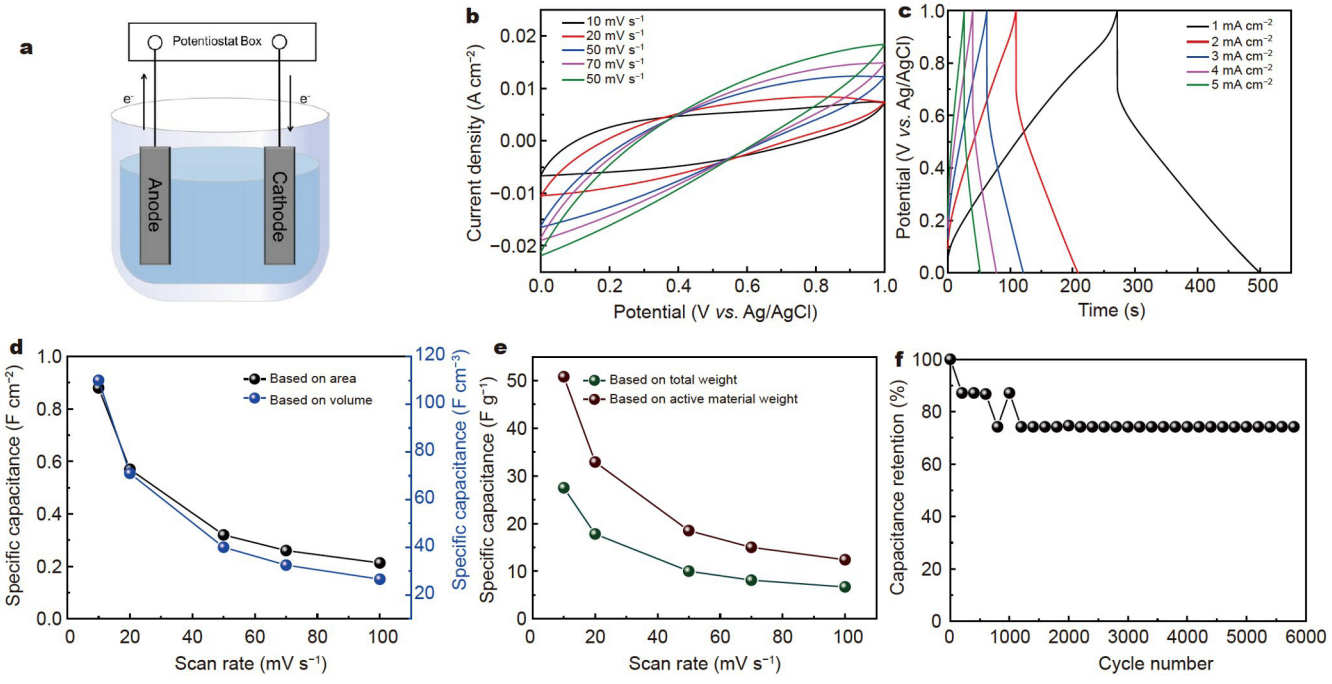

Figure 7 (a) Schematic illustration of the PPy:PSS/CNP supercapacitor device; (b) CV curves at different scan rates; (c) GCD curves at different current densities; (d) specific capacitance based on area and volume; (e) specific capacitance based on total weight and active material weight; (f) cycling stability at 5 mA cm^{-2}.

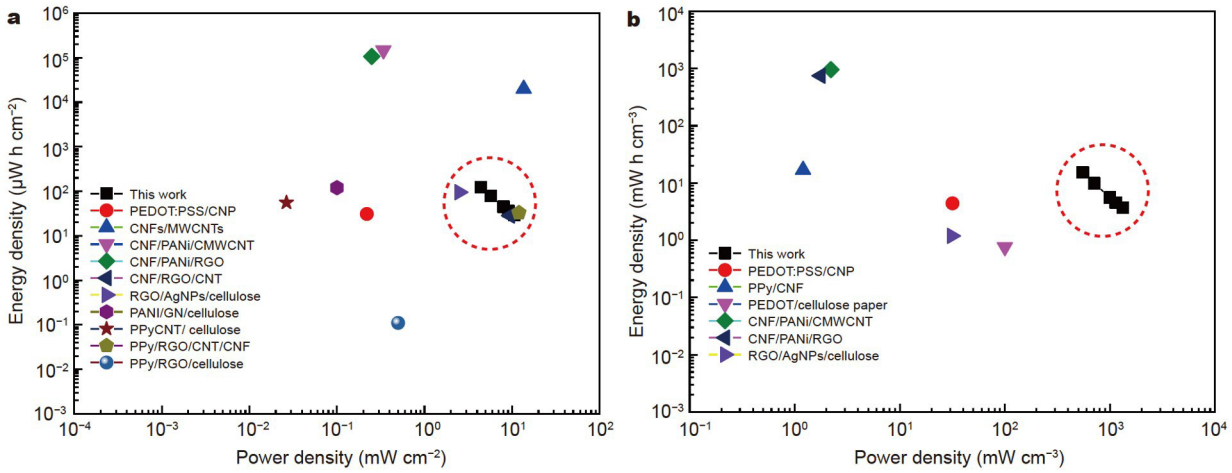

Figure 8 Ragone plots of the symmetrical PPy:PSS/CNP supercapacitor device based on (a) area and (b) volume in comparison with other devices based on cellulose materials.

The symmetric device exhibited the symmetrical shape of CV curves and negligible deformations with the increasing scan rates, indicating the ideal capacitive, excellent rate feature, and good reversibility (Fig. 7b). GCD curves displayed a nearly triangle shape with low voltage drops, which further proved a typical electric double layer capacitor (EDLC) nature of energy storage (Fig. 7c). In addition, as the current density increased, the shape of the GCD curves remained, indicating that the device had good redox reversibility. The capacitance values of PPy:PSS/CNP-4 device based on area, volume, and weight were plotted in Fig. 7d, e to evaluate the performance of supercapacitors. At 10 mV s^{-1}, the maximum areal capacitance was 880 mF cm^{-2} (110 F cm^{-3}, 50.8 F g^{-1}). The results of the cyclic performance indicated that the device showed 74% capacitance retention after 5800 cycles at 5 mA cm^{-2} (Fig. 7f). As shown in the Ragone plots (Fig. 8), the maximum energy density can reach 122 μW h cm^{-2} (15 W h cm^{-3}) with the power density of 4.4 mW cm^{-2} (550 mW cm^{-3}), which was comparable to or even higher than the previous supercapacitor devices based on similar cellulose materials, demonstrating the satisfied electrochemical performance [40–49]. The impressive findings suggested that PPy:PSS/CNP was a promising material for high-performance energy storage devices.

CONCLUSIONS

In this study, a low-cost and environmentally friendly nanocellulose was used as building blocks for PPy:PSS to fabricate the freestanding, binder-free flexible PPy:PSS/CNP electrode using the vacuum filtration method. Due to the synergistic effect of three constituents, the PPy:PSS/CNP exhibited excellent flexibility and outstanding electrochemical properties. When the weight percentage of PPy:PSS in PPy:PSS/CNP was 54.1%, the electrode exhibited the maximum specific capacitance value (3.8 F cm^{-2}, 475 F cm^{-3}, 240 F g^{-1}, at 10 mV s^{-1}) and good cycling stability (80.9% capacitance retention after 5000 cycles). The good flexibility and electrochemical stability of the electrode were proved by the CV measurements of PPy:PSS/CNP at different bending angles. Furthermore, the symmetric supercapacitor device based on PPy:PSS/CNP was assembled, which offered the highest areal energy density of 122 μW h cm^{-2} (15 W h cm^{-3}) along with the power density of 4.4 mW cm^{-2} (550 mW cm^{-3}). Our work provides a novel design idea to synthesize free-standing flexible nanopaper electrodes with good mechanical strength and electrochemical performance for future energy storage applications. Moreover, the simple and economical preparation process may bring new opportunities in reducing the production cost of flexible electrodes for portable and wearable consumer electronics.

Received 20 June 2022; accepted 8 August 2022; published online 2 November 2022

1 Poonam , Sharma K, Arora A, *et al*. Review of supercapacitors: Materials and devices. J Energy Storage, 2019, 21: 801–825
2 Wang G, Zhang L, Zhang J. A review of electrode materials for electrochemical supercapacitors. Chem Soc Rev, 2012, 41: 797–828
3 Wang Y, Wu X, Han Y, *et al*. Flexible supercapacitor: Overview and outlooks. J Energy Storage, 2021, 42: 103053
4 Chee WK, Lim HN, Zainal Z, *et al*. Flexible graphene-based supercapacitors: A review. J Phys Chem C, 2016, 120: 4153–4172
5 Hillier N, Yong S, Beeby S. The good, the bad and the porous: A review of carbonaceous materials for flexible supercapacitor applications. Energy Rep, 2020, 6: 148–156
6 Huang Y, Li H, Wang Z, *et al*. Nanostructured polypyrrole as a flexible electrode material of supercapacitor. Nano Energy, 2016, 22: 422–438
7 Yi TF, Qiu LY, Mei J, *et al*. Porous spherical NiO@$NiMoO_4$@PPy nanoarchitectures as advanced electrochemical pseudocapacitor materials. Sci Bull, 2020, 65: 546–556
8 Fu H, Du Z, Zou W, *et al*. Carbon nanotube reinforced polypyrrole nanowire network as a high-performance supercapacitor electrode. J Mater Chem A, 2013, 1: 14943
9 Qian T, Yu C, Wu S, *et al*. A facilely prepared polypyrrole-reduced graphene oxide composite with a crumpled surface for high performance supercapacitor electrodes. J Mater Chem A, 2013, 1: 6539
10 Gahlout P, Choudhary V. Tailoring of polypyrrole backbone by optimizing synthesis parameters for efficient EMI shielding properties in X-band (8.2–12.4 GHz). Synth Met, 2016, 222: 170–179
11 Huang YM, Zhou F, Deng Y, *et al*. Effects of salt 9,10-anthraquinone-2-sulfonic acid sodium on the conductivity of polypyrrole. Solid State Ion, 2008, 179: 1305–1309
12 Wang W, Li Z, Jiang T, *et al*. Sulfonated poly(ether ether ketone)/polypyrrole core-shell nanofibers: A novel polymeric adsorbent/conducting polymer nanostructures for ultrasensitive gas sensors. ACS Appl Mater Interfaces, 2012, 4: 6080–6084
13 Malik RS, Tripathi SN, Gupta D, *et al*. Novel anhydrous composite membranes based on sulfonated poly(ether ketone) and aprotic ionic

liquids for high temperature polymer electrolyte membranes for fuel cell applications. Int J Hydrogen Energy, 2014, 39: 12826–12834
14 Ouyang J, Chu CW, Chen FC, *et al.* High-conductivity poly(3,4-ethylenedioxythiophene):poly(styrene sulfonate) film and its application in polymer optoelectronic devices. Adv Funct Mater, 2005, 15: 203–208
15 Maruthamuthu S, Chandrasekaran J, Manoharan D, *et al.* Conductivity and dielectric analysis of nanocolloidal polypyrrole particles functionalized with higher weight percentage of poly(styrene sulfonate) using the dispersion polymerization method. J Polym Eng, 2017, 37: 481–492
16 Miao C, Du H, Zhang X, *et al.* Dynamic crack initiation and growth in cellulose nanopaper. Cellulose, 2021, 29: 557–569
17 Liu H, Du H, Zheng T, *et al.* Cellulose based composite foams and aerogels for advanced energy storage devices. Chem Eng J, 2021, 426: 130817
18 Zhao D, Zhang Q, Chen W, *et al.* Highly flexible and conductive cellulose-mediated PEDOT:PSS/MWCNT composite films for supercapacitor electrodes. ACS Appl Mater Interfaces, 2017, 9: 13213–13222
19 Jyothibasu JP, Kuo DW, Lee RH. Flexible and freestanding electrodes based on polypyrrole/carbon nanotube/cellulose composites for supercapacitor application. Cellulose, 2019, 26: 4495–4513
20 Du H, Zhang M, Liu K, *et al.* Conductive PEDOT:PSS/cellulose nanofibril paper electrodes for flexible supercapacitors with superior areal capacitance and cycling stability. Chem Eng J, 2022, 428: 131994
21 Parit M, Du H, Zhang X, *et al.* Polypyrrole and cellulose nanofiber based composite films with improved physical and electrical properties for electromagnetic shielding applications. Carbohydrate Polyms, 2020, 240: 116304
22 Li S, Shi Q, Li Y, *et al.* Intercalation of metal ions into $Ti_3C_2T_x$ MXene electrodes for high-areal-capacitance microsupercapacitors with neutral multivalent electrolytes. Adv Funct Mater, 2020, 30: 2003721
23 Wan C, Jiao Y, Li J. Flexible, highly conductive, and free-standing reduced graphene oxide/polypyrrole/cellulose hybrid papers for supercapacitor electrodes. J Mater Chem A, 2017, 5: 3819–3831
24 Maruthamuthu S, Chandrasekaran J, Manoharan D, *et al.* Effect of $CuBr_2$ salt treatment on the performance of nanocolloidal PPy:PSS multilayer thin film counter electrodes of dye-sensitized solar cells. J Appl Polym Sci, 2016, 133: 43114
25 Lay M, Pèlach MÀ, Pellicer N, *et al.* Smart nanopaper based on cellulose nanofibers with hybrid PEDOT:PSS/polypyrrole for energy storage devices. Carbohydrate Polyms, 2017, 165: 86–95
26 Fei X, Wang J, Zhu J, *et al.* Biobased poly(ethylene 2,5-furancoate): No longer an alternative, but an irreplaceable polyester in the polymer industry. ACS Sustain Chem Eng, 2020, 8: 8471–8485
27 Fei G, Wang Y, Wang H, *et al.* Fabrication of bacterial cellulose/polyaniline nanocomposite paper with excellent conductivity, strength, and flexibility. ACS Sustain Chem Eng, 2019, 7: 8215–8225
28 Li Y, Zhang H, Ni S, *et al. In situ* synthesis of conductive nanocrystal cellulose/polypyrrole composite hydrogel based on semi-interpenetrating network. Mater Lett, 2018, 232: 175–178
29 Kashani H, Chen L, Ito Y, *et al.* Bicontinuous nanotubular graphene-polypyrrole hybrid for high performance flexible supercapacitors. Nano Energy, 2016, 19: 391–400
30 Zhang J, Chen P, Oh BHL, *et al.* High capacitive performance of flexible and binder-free graphene-polypyrrole composite membrane based on *in situ* reduction of graphene oxide and self-assembly. Nanoscale, 2013, 5: 9860–9866
31 Guan X, Pan L, Fan Z. Flexible, transparent and highly conductive polymer film electrodes for all-solid-state transparent supercapacitor applications. Membranes, 2021, 11: 788
32 Du H, Parit M, Liu K, *et al.* Engineering cellulose nanopaper with water resistant, antibacterial, and improved barrier properties by impregnation of chitosan and the followed halogenation. Carbohydrate Polyms, 2021, 270: 118372
33 Miao F, Shao C, Li X, *et al.* Electrospun carbon nanofibers/carbon nanotubes/polyaniline ternary composites with enhanced electrochemical performance for flexible solid-state supercapacitors. ACS Sustain Chem Eng, 2016, 4: 1689–1696
34 Xia L, Li X, Wu Y, *et al.* Electrodes derived from carbon fiber-reinforced cellulose nanofiber/multiwalled carbon nanotube hybrid aerogels for high-energy flexible asymmetric supercapacitors. Chem Eng J, 2020, 379: 122325
35 Hou M, Xu M, Hu Y, *et al.* Nanocellulose incorporated graphene/polypyrrole film with a sandwich-like architecture for preparing flexible supercapacitor electrodes. Electrochim Acta, 2019, 313: 245–254
36 Olsson H, Nyström G, Strømme M, *et al.* Cycling stability and self-protective properties of a paper-based polypyrrole energy storage device. Electrochem Commun, 2011, 13: 869–871
37 Koga H, Tonomura H, Nogi M, *et al.* Fast, scalable, and eco-friendly fabrication of an energy storage paper electrode. Green Chem, 2016, 18: 1117–1124
38 Anothumakkool B, Soni R, Bhange SN, *et al.* Novel scalable synthesis of highly conducting and robust PEDOT paper for a high performance flexible solid supercapacitor. Energy Environ Sci, 2015, 8: 1339–1347
39 Wang T, Zhang W, Yang S, *et al.* Preparation of foam-like network structure of polypyrrole/graphene composite particles based on cellulose nanofibrils as electrode material. ACS Omega, 2020, 5: 4778–4786
40 Fu Q, Wang Y, Liang S, *et al.* High-performance flexible freestanding polypyrrole-coated CNF film electrodes for all-solid-state supercapacitors. J Solid State Electrochem, 2020, 24: 533–544
41 Li B, Lopez-Beltran H, Siu C, *et al.* Vaper phase polymerized PEDOT/cellulose paper composite for flexible solid-state supercapacitor. ACS Appl Energy Mater, 2020, 3: 1559–1568
42 Gao K, Shao Z, Wang X, *et al.* Cellulose nanofibers/multi-walled carbon nanotube nanohybrid aerogel for all-solid-state flexible supercapacitors. RSC Adv, 2013, 3: 15058
43 Lyu S, Chen Y, Zhang L, *et al.* Nanocellulose supported hierarchical structured polyaniline/nanocarbon nanocomposite electrode *via* layer-by-layer assembly for green flexible supercapacitors. RSC Adv, 2019, 9: 17824–17834
44 Zheng Q, Cai Z, Ma Z, *et al.* Cellulose nanofibril/reduced graphene oxide/carbon nanotube hybrid aerogels for highly flexible and all-solid-state supercapacitors. ACS Appl Mater Interfaces, 2015, 7: 3263–3271
45 Zou Z, Zhou W, Zhang Y, *et al.* High-performance flexible all-solid-state supercapacitor constructed by free-standing cellulose/reduced graphene oxide/silver nanoparticles composite film. Chem Eng J, 2019, 357: 45–55
46 Liu R, Ma L, Huang S, *et al.* A flexible polyaniline/graphene/bacterial cellulose supercapacitor electrode. New J Chem, 2017, 41: 857–864
47 Wang W, Yang Y, Chen Z, *et al.* High-performance yarn supercapacitor based on directly twisted carbon nanotube@bacterial cellulose membrane. Cellulose, 2020, 27: 7649–7661
48 Bai Y, Liu R, Li E, *et al.* Graphene/carbon nanotube/bacterial cellulose assisted supporting for polypyrrole towards flexible supercapacitor applications. J Alloys Compd, 2019, 777: 524–530
49 Ma L, Liu R, Niu H, *et al.* Flexible and freestanding electrode based on polypyrrole/graphene/bacterial cellulose paper for supercapacitor. Compos Sci Tech, 2016, 137: 87–93

Acknowledgements This work was partially supported by the National Science Foundation (CMMI-2113948). Liang Y acknowledges the financial support from China Scholarship Council (201708510080).

Author contributions Zhang X conceived the idea. Liang Y designed and performed the experiments with the help from Wang HE. Wei Z performed the SEM test. Liang Y analyzed the data and drafted the manuscript. Zhang X and Wang R supervised the whole research. All authors participated in the general discussion.

Conflict of interest The authors declare that they have no conflict of interest.

Supplementary information Supporting data are available in the online version of the paper.

Yue Liang received her master's degree from China West Normal University in June 2017. Since 2018, she has been studying as a doctoral candidate in the group of Prof. Xinyu Zhang at the Department of Chemical Engineering, Auburn University. Her research interests mainly focus on microwave-initiated ultrafast nanomanufacturing for hierarchical, multifunctional nanomaterials and nanocomposites, and the fabrication of flexible electrodes based on conducting polymers.

Ruigang Wang received his doctorate with Prof. Peter Crozier and Dr. Renu Sharma in materials science and engineering from Arizona State University in 2007. In August 2016, he joined the Department of Metallurgical and Materials Engineering, The University of Alabama as an associate professor. His research mainly focuses on shape/size-controlled synthesis of metal oxides, emission control catalysts, support structure effect in metal-oxide catalysis, materials for energy capture, storage and conversion, metal recycling, and high temperature ceramics processing.

Xinyu Zhang received his doctorate with Prof. Alan G. MacDiarmid and Dr. Sanjeev K. Manohar in materials chemistry from the University of Texas at Dallas in 2005. He is a professor in chemical engineering at Auburn University and his research mainly focuses on microwave-initiated ultrafast nanomanufacturing for hierarchical, multifunctional nanomaterials and nanocomposites, multifunctional polymer coating for anti-corrosion and antimicrobial applications, and green approach to conducting polymer-based nanocomposites for catalysis, sensing and energy storage applications.

基于PPy:PSS纳米纤维素复合材料的高性能柔性独立导电纳米纸用于超级电容器

梁月[1], 魏震[2], 王鸿恩[1], 王瑞刚[2*], 张新宇[1*]

摘要 本工作通过低成本、简单、快速的真空过滤方法首次成功制备了一种独立的、无粘合剂的柔性聚吡咯:聚磺苯乙烯/纤维素纳米纸电极(PPy:PSS/CNP). 多层结构的纤维素纳米纸具有较高的表面积和良好的机械强度, 不仅提供了高的电活性区域, 缩短了电解质离子的扩散距离, 而且还阻止了PPy在充电/放电过程中的体积膨胀/收缩. 优化后的PPy:PSS/CNP在10 mV s^{-1}时表现出3.8 F cm^{-2} (对应于475 F cm^{-3}和240 F g^{-1})的高比电容和良好的循环稳定性(在5000次循环后有80.9%的电容保持率). PPy:PSS/CNP在不同弯曲角度下的循环伏安曲线表明电极具有突出的柔韧性和电化学稳定性. 此外, 组装的对称超级电容器器件在功率密度为4.4 mW cm^{-2} (550 mW cm^{-3})的情况下, 提供了122 μW h cm^{-2} (15 W h cm^{-3})的高面积能量密度, 这个值优于其他基于纤维素电极材料制备的器件. PPy:PSS/CNP电极结合了高电容性能、灵活性、易于制造和廉价多个优势, 为开发下一代绿色、经济便携式和可穿戴电子产品提供了巨大潜力.

